VOLUME 112, NUMBER 16
AUGUST 1, 1990

JOURNAL
OF THE
AMERICAN
CHEMICAL
SOCIETY

Differential Conformational Mobilities on Different Time Scales in B- and Z-DNA Oligomers in Solution

Satoshi Ikuta* and Yu-Sen Wang†

Contribution from the Department of Chemistry, Illinois Institute of Technology, Chicago, Illinois 60616. *Received July 3, 1989*

Abstract: Measurements of $T_{1\rho}$ in solution are well suited for detection of molecular dynamics of biological macromolecules on a microsecond time scale. We present an analysis of on-resonance proton rotating frame spin–lattice relaxation ($T_{1\rho}$) measurements for the B and Z family of duplexes d(CGCGCG) [B-d(CG)$_3$ and Z-d(CG)$_3$] in solution. The results obtained from a $T_{1\rho}$ analysis are compared with those from NOE experiments. Measurements of $T_{1\rho}$ for the H5 of the cytosine protons (CH5) indicate that Z-d(CG)$_3$ is more conformationally mobile than B-d(CG)$_3$. However, pre-steady-state NOE experiments indicate that the reverse is true. Each technique detects conformational exchanges occurring on a characteristic time scale: the microsecond time scale by $T_{1\rho}$ and the nanosecond time scale by NOE. These data clearly demonstrate that B- and Z-d(CG)$_3$ each possess different internal mobilities on the different time scales.

Introduction

The importance of internal mobilities in biological macromolecules has been long recognized. Along this line, NMR techniques have successfully been utilized to investigate DNA dynamics in solution.[1-3] For modern high-resolution NMR spectrometers with ^{1}H nuclei, T_1 and NOE measurements are sensitive to kinetics on the nanosecond time scale, and T_2 and line shape analysis are affected by (chemical exchange) processes that occur in the millisecond time domain. The microsecond time scale dynamics of DNA and other macromolecules in solution cannot readily be examined by conventional solution NMR techniques, except by an off-resonance rotating frame spin–lattice relaxation ($T_{1\rho}^{off}$) experiment developed by James and co-workers.[2a]

In contrast, an on-resonance proton rotating frame spin–lattice relaxaton, $T_{1\rho}$, measurement detects molecular dynamics occurring in solution on a time scale near the inverse of the frequency of the spin-locking field, ω_1 (thousands of hertz), corresponding to the microsecond time scale. Measurements of $T_{1\rho}$ have previously been used to monitor the dynamics of small[4-6] and intermediate size molecules.[7,8] However, these techniques have not yet been applied to studies of the dynamics of large molecules in solution because of the complexity of interpreting the $T_{1\rho}$ relaxation data.

We recently proposed a procedure for the analysis of $T_{1\rho}$ relaxation data for macromolecules[9] and examined the accuracy of the dynamics obtained by $T_{1\rho}$ measurements using well-characterized systems.[10] We now report an application to a study of the conformational exchange within B- and Z-type oligodeoxyribonucleotide on the microsecond time scale. We compare

* Author to whom correspondence should be addressed.
† Present address: Department of Chemistry and Biochemistry, University of Maryland, College Park, MD 20742.

(1) Jardetzky, O. *Acc. Chem. Res.* **1981**, *14*, 291–298.
(2) (a) Bolton, P. H.; James, T. L. *J. Am. Chem. Soc.* **1980**, *102*, 25–31. (b) Mirau, P. A.; Behling, R. W.; Kearns, D. R. *Biochemistry* **1985**, *24*, 6200–6211. (c) Shindo, H.; Hiyama, Y.; Roy, S.; Cohen, J. S.; Torchia, D. A. *Bull. Chem. Soc. Jpn.* **1987**, *60*, 1631–1640.
(3) (a) Kintanar, A.; Huang, W.-H.; Schindele, D. C.; Wemmer, D. E.; Drobny, G. *Biochemistry* **1989**, *28*, 282–293. (b) Brandes, R.; Vold, R. R.; Vold, R. L.; Kearns, D. R. *Biochemistry* **1986**, *25*, 7744–7751.
(4) Strange, J. H.; Morgan, R. E. *J. Phys. C* **1970**, *3*, 1999–2011.
(5) Deverell, C.; Morgan, R. E.; Strange, J. H. *Mol. Phys.* **1979**, *18*, 553–559.
(6) (a) Bleich, H. E.; Glasel, J. A. *Biopolymers* **1978**, *17*, 2445–2457. (b) Bleich, H. E.; Day, A. R.; Freer, R. J.; Glasel, J. A. *Biochem. Biophys. Res. Commun.* **1979**, *87*, 1146–1153.
(7) Kopple, K. D.; Bhandary, K. K.; Kartha, G.; Wang, Y.-S.; Parameswaran, K. N. *J. Am. Chem. Soc.* **1986**, *108*, 4637–4642.
(8) Kopple, K. D.; Wang, Y.-S.; Cheng, A. G.; Bhandary, K. K. *J. Am. Chem. Soc.* **1988**, *110*, 4168–4176.
(9) Wang, Y.-S.; Ikuta, S. *J. Am. Chem. Soc.* **1989**, *111*, 1243–1248.
(10) Wang, Y.-S.; Ikuta, S. *Magn. Reson. Chem.* **1989**, *27*, 1134–1141.

0002-7863/90/1512-5901$02.50/0

the microsecond conformational exchange detected by $T_{1\rho}$ measurements with those on the nanosecond time scale which we monitored with pre-steady-state NOE measurements.

Experimental Section

Materials. A hexamer d(CGCGCG), henceforth referred to as d-$(CG)_3$, was prepared by the published procedure.[11] The NMR sample was comprised of ~3.6 mg of $d(CG)_3$ dissolved in 0.3 mL of D_2O (4.2 mM strand concentration) containing 10 mM phosphate buffer, 0.1 M NaCl, and 2 M $NaClO_4$ at pH = 6.6, in a 5 mm NMR tube.

NMR Measurements. NMR spectra and relaxation data were obtained on a Nicolet NT-300 spectrometer. Selective spin–lattice relaxation experiments were carried out following a selective 180° soft pulse (26 ms) from the decoupler to the signals of interest. Nuclear Overhauser Effects (NOE) were recorded by one-dimensional difference spectroscopy. Irradiation of an envelop of H6 of cytosines, CH6, at different time periods resulted in NOEs on H5 of cytosines, CH5. In order to determine cross-relaxation rates, σ, from the NOE data, a spectral region of interest (CH5) in the difference spectra are expanded and plotted. Peak areas, instead of peak intensities, were counted to measure the NOE enhancement. Assignments of the signals to the specific protons were carried out by the standard procedure.[12,13]

Rotating frame spin–lattice relaxation times, $T_{1\rho}$, were measured by the procedure described previously.[9] The peak intensities were fitted to $I = I_0 \exp[-t/T_{1\rho}] + I_p$, where I_p is the residual signal at long spin-locking times, by a nonlinear least-squares analysis to obtain $T_{1\rho}$ $(1/R_{1\rho})$. The spin-locking was achieved at radio frequency fields ranging from 2212 to 7463 Hz. We used low power pulse for both spin-locking and 90° pulses. Calibration of spin-locking fields, $\omega_1 = \gamma B_1$, was made by finding accurate 360° pulse lengths. The carrier frequency was placed in the middle of the signals of interest within 100 Hz. There was no observable change in the $T_{1\rho}$ relaxation time between an exact on-resonance and an off-resonance within 100 Hz. The spin-locking experiments generated heat, for example ω_1 = 10000 Hz corresponded to heat generation of ~2 W. To find out the effect of heat generation on the sample temperature during the spin-locking, the temperature was measured with use of methanol[14] and a sample that contains 2 M $NaClO_4$, 0.1 M NaCl, and 10 mM phosphate buffer at pH = 6.6. We found no change in the temperature of the sample during the spin-locking experiments.

Analysis of $T_{1\rho}$ Data. An analysis of $T_{1\rho}$ data is similar to that previously published,[9] however, we introduce a few modifications and improvements. For a proton directly attached to a carbon atom (C–H), the major relaxation mechanism to the observed relaxation rates in the rotating frame, $R_{1\rho(obs)}$, is the dipole–dipole interaction, $R_{1\rho(dd)}$. An additional relaxation mechanism to $R_{1\rho(obs)}$ is the contribution from the conformational exchange, $R_{1\rho(ex)}$. $R_{1\rho(ex)}$ is expressed as

$$R_{1\rho(exch)} = R_{1\rho(obs)} - R_{1\rho(dd)} \quad (1)$$

and a ratio is defined as

$$\text{ratio}^{15} = R_{1\rho(dd)}/R_{1(dd)} \text{ (for a non-spin-diffusion case)} \quad (2')$$

or

$$\text{ratio} = R_{1\rho(dd)}/R_1{}^{IS}{}_{(dd)} \text{ (for a spin-diffusion case)} \quad (2)$$

where $R_1{}^{IS}{}_{(dd)}$ is the initial recovery of selective spin–lattice relaxation measurements. The dipolar, quadrupolar, and scalar interactions contribute to relaxation mechanisms of $T_{1\rho}$, T_1, and T_2 equally for small molecules with $\omega_0\tau_c \ll 1$[5] where τ_c is a correlation time for molecular tumbling and ω_0 is the Larmor frequency. In other words, the ratio between $R_{1\rho(dd)}$ and $R_{1(dd)}$ is unity in the case of extreme narrowing conditions.[9] However, for larger molecules with $\omega_0\tau_c \geq 1$, $R_{1\rho(dd)}$ differs from $R_{1(dd)}$. Therefore, the ratio between $R_{1\rho(dd)}$ and $R_{1(dd)}$ must be known to evaluate $R_{1\rho(exch)}$.[9]

We calculated the ratio $[R_{1\rho(dd)}/R_{1(dd)}]$ using an overall tumbling time of the molecule, τ_c, in the previous study.[9] In this study, we used an improved procedure. It is still essential to use the correlation time of $d(CG)_3$ on the nanosecond time scale for computing the ratio, $R_{1\rho(dd)}$, and $R_{1\rho(exch)}$. The correlation time may vary at different parts of molecules due to the presence of conformational exchange (internal motions).

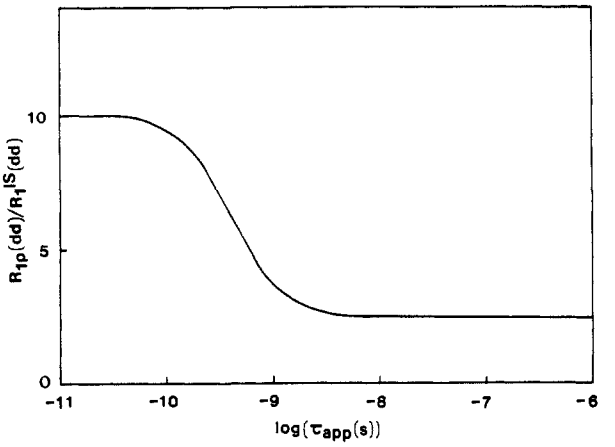

Figure 1. Theoretical values of the ratios $[R_{1\rho(dd)}/R_1{}^{IS}{}_{(dd)}]$ at constant field strengths, γB_0 = 300 MHz and γB_1 = 5000 Hz as a function of τ_{app} (see ref 9).

Therefore, the ratio $[R_{1\rho(dd)}/R_{1(dd)}]$ or $[R_{1\rho(dd)}/R_1{}^{IS}{}_{(dd)}]$ should be best evaluated by using the local correlation time, τ_{eff}, which includes the effect of the overall tumbling time of the molecule and the local conformational exhcanges (internal motions). We carried out pre-steady-state NOE experiments to determine cross-relaxation rates, σ, of the CH6→CH5 vector, and obtained an apparent correlation time, τ_{app}, which was used as the local correlation time, τ_{eff}. The CH6→CH5 is the same spin system used for $T_{1\rho}$ measurements. From the τ_{eff} (or τ_{app}) value, the ratio is calculated, leading to $R_{1\rho(dd)}$ and $R_{1\rho(exch)}$. This is the main difference in the procedure to evaluate $R_{1\rho(exch)}$ between this study and the previous study.[9] It should be noted that the CH6→CH5 (i) has a fixed interproton distance and (ii) is the most appropriate spin system to provide the local correlation time, τ_{eff}, of the signal of interest, CH5.

The protocol for the $T_{1\rho}$ relaxation studies of short oligonucleotides with $\omega_0\tau_c > 1$ is as follows: 1. Measurements of $T_{1\rho}$ for the CH5 yield $R_{1\rho(obs)}$. 2. Measurements of initial recovery of selective spin–lattice relaxation for the CH5 yield $R_1{}^{IS}{}_{(obs)}$. 3. Measurements of pre-steady-state NOE of the CH5–CH6 vector yield the apparent correlation time, τ_{app}, which includes contributions from an overall tumbling and an internal molecular motion (see below). 4. The ratio = $R_{1\rho(dd)}/R_1{}^{IS}{}_{(dd)}$ in eq 2 (see ref 9 and 15) is obtained from the τ_{eff} (τ_{app}) values (see Figure 1). 5. $R_{1\rho(dd)}$ is obtained as a product of the ratio and $R_1{}^{IS}{}_{(obs)}$. 6. $R_{1\rho(exch)}$ is the difference between $R_{1\rho(obs)}$ and $R_{1\rho(dd)}$ (see eq 1).

Regarding the procedure to extract $R_{1\rho(dd)}$, two points should be mentioned. (i) τ_{app} contributes to dipolar terms in both rotating and laboratory frame relaxation rates. In principle the existence of microsecond and nanosecond molecular events modifies the spectral densities of $R_{1\rho(dd)}$ and $R_{1(dd)}$. For example, the contributions of the microsecond conformational exchanges to the spectral density of $T_{1\rho}$ and T_1 were calculated by using $J(\omega_0) = (1/5)\tau_{exch}[1 + (\omega_0\tau_{exch})^2]^{-1}$ where ω_0 = 300 MHz and τ_{exch} = 1 μs and 1 ns, respectively. The calculation showed that the contribution of the microsecond conformational exchanges to T_1 relaxation is 770 times smaller than that to $T_{1\rho}$: the conformational exchange occurring on the time scale of $1/\omega_1$ contributes practically only to rotating frame relaxation rates but not to those of laboratory frame relaxation rates. This is the reason that the ratio calculated from τ_{app} and the experimentally obtained $R_1{}^{IS}{}_{(obs)}$ are used to evaluate $R_{1\rho(dd)}$. (iii) Although a two-spin system is used to derive the equation for the ratio $R_{1\rho(dd)}/R_{1(dd)}$ in the previous paper,[9] the result is also valid for a multispin system. The value of the ratio for the two-spin system is identical with that of a multispin system as long as a single correlation time, τ_{app}, is used.

An analysis of exchange contributions, $R_{1\rho(exch)}$, is made from a model in which spins are exchanging between sites A and B with equal population. In this case $R_1 << \sigma ho_{(exch)}$ is expressed as[5]

$$R_{1\rho(exch)} = 1/T_{1\rho(exch)} = (\Delta\omega)^2\tau_{exch}/[4(1 + \omega_1{}^2\tau_{exch}{}^2)] \quad (3)$$

where ω_1 is the spin-locking frequency, τ_{exch} is the lifetime of the conformational exchange, and $\Delta\omega = \omega_A - \omega_B$ is the chemical shift difference between the two exchanging species, ω_A and ω_B. Equation 3 indicates that (i) the exchange contribution, $R_{1\rho(exch)}$, will be maximal at $\tau_{exch} = 1/\omega_1$, and (ii) values of τ_{exch} and $\Delta\omega$ may be extended from a plot of $T_{1\rho(exch)}$ against $\omega_1{}^2$ in an appropriate case.

(11) Tan, Z. K.; Ikuta, S.; Haung, T.; Dugaiczyk, A.; Itakura, K. *Cold Spring Harbor Symp. Quant. Biol.* **1983**, *47*, 383–391.
(12) Kumar, A.; Ernst, R. R.; Wuthrich, K. *Biochem. Biophys. Res. Commun.* **1980**, *95*, 1.
(13) Nagayama, K.; Kumar, A.; Wuthrich, K.; Ernst, R. R. *J. Magn. Reson.* **1980**, *40*, 321.
(14) Van Geet, A. L. *Anal. Chem.* **1968**, *40*, 2227–2229.

(15) $R_{1\rho(dd)} = (\hbar^2\gamma_H{}^2\gamma_1{}^2)/4r^6[4J(\omega_1) + J_0(\omega_H - \omega_1) + 3J_1(\omega_H) + 6J_1(\omega_1) + 6J_2(\omega_H + \omega_1)]$, $R_1{}^{IS} = (\hbar^2\gamma_H{}^2\gamma_{I2})2r^6/[J_0(\omega_H - \omega_1)]$, and $J_n(\omega_0) = (\tau_{app}/5)[1 + (\omega_0\tau_{app})^2]^{-1}$; see more details in the references of ref 9.

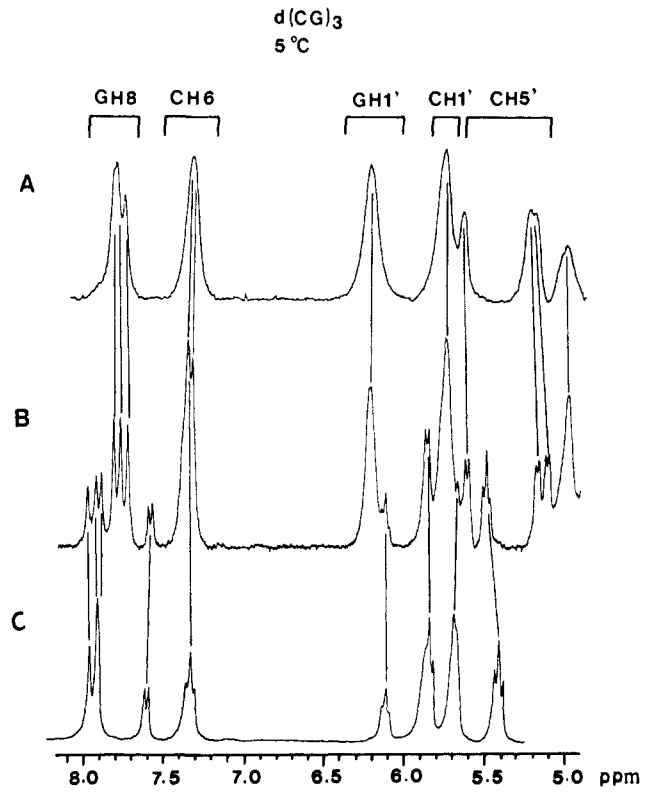

Figure 2. ^{1}H NMR spectra of the nonexchangeable protons in d(CG)$_3$ at 5 °C in D_2O: (A) the spectrum of d(CG)$_3$ in 4 M $NaClO_4$, (B) the spectrum of d(CG)$_3$ in 2 M $NaClO_4$, (C) the spectrum of d(CG)$_3$ in 0 M $NaClO_4$.

Analysis of NOE Data. The initial slope of NOE enhancement of two spins i and j, N_{ij}, is related to the cross-relaxation rates, σ, and the apparent correlation time, τ_{app}, as follows.[16,17]

$$\mathrm{NOE}_{ij}(t) = \sigma t \tag{4}$$

$$\sigma_{ij} = K[J(0) - 6J(2\omega_0)] = (K/5)[\tau_{app} - 6\tau_{app}/(1 + 4\tau_{app}^2\omega_0^2)] \tag{5}$$

where $K = (h^2\gamma_H^2\gamma_I^2)/2r^6$, r is the i–j internuclear distance, h is Planck's constant divided by 2π, ω_0 is the Larmor frequency of spins, and t is the irradiation time. With a fixed interpretation distance, r_{ij} = 2.46 Å, for the CH5→CH6 on the basis of standard bond lengths and angles, τ_{app} is readily extracted.[18]

Results

Coexistence of B- and Z-d(CG)$_3$. Figure 2 shows spectra of nonexchangeable proton signals of d(CG)$_3$ in 0, 2, and 4 M $NaClO_4$ solutions at 5 °C. Two sets of signals of d(CG)$_3$ in 2 M $NaClO_4$ correspond to those of 0 and 4 M $NaClO_4$, respectively, though subtle changes are seen in the chemical shift of GH8 and CH5 signals. The following evidence confirms that d(CG)$_3$ in 2 M $NaClO_4$ exists mainly as the B- and Z-family of double helices. (i) UV melting experiments were carried out, and transition midpoints, T_m, of d(CG)$_3$ at 5μM strand concentration were 43 and 23 °C in 0 and 4 M $NaClO_4$, respectively,[19a] while T_m at 1.6 mM strand concentration in 0 M $NaClO_4$ was 67 °C.[19b] (ii) Circular dichroism (CD) spectra were recorded for d(CG)$_3$ in 0 and 4 M $NaClO_4$. We observed the spectral inversion of d(CG)$_3$ in 4 M $NaClO_4$ in Figure 2B of ref 19a. CD spectra indicate d(CG)$_3$ exists as duplexes. (iii) 1- and 2-D NOE experiments were carried out for d(CG)$_3$ in 0, 4, and 2 M $NaClO_4$.

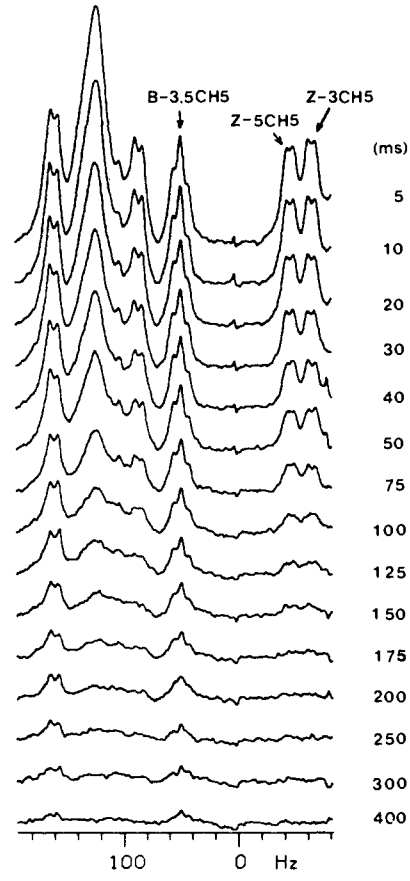

Figure 3. Rotating frame spin–lattice relaxation measurement on the 3/5CH5 in B- and Z-d(CG)$_3$ at 0 °C with ω_1 = 7463 Hz. d(CG)$_3$ has 4.2 mM strand concentration in 10 mM phosphate buffer, 0.1 M NaCl and 2 M $NaClO_4$, at pH = 6.6.

Table I. Laboratory Frame Relaxation Rates[a] ($R_1^{IS}{}_{(obs)}$), Cross-Relaxation Rates (σ), and Apparent Correlation Times (τ_{app}) of B- and Z-d(CG)$_3$ in 2 M $NaClO_4$ at 5 and 0 °C

	σ, s^{-1}	τ_{app}, ns	ratio	$R_1^{IS}{}_{(obs)}$, s^{-1}	$R_{1\rho(dd)}$, s^{-1}
		5 °C			
B-d(CG)$_3$ 3/5CH5	0.4	1.7	3.0	3.0	9.0
Z-d(CG)$_3$ 3CH5	0.9	3.6	2.6	5.0	13.0
Z-d(CG)$_3$ 5CH5	0.9	3.6	2.6	5.3	13.8
		0 °C			
B-d(CG)$_3$ 3/5CH5	0.6	2.6	2.7	4.0	10.8
Z-d(CG)$_3$ 3/CH5	1.1	4.4	2.6	6.3	16.4
Z-d(CG)$_3$ 5/CH5	1.1	4.4	2.6	6.6	17.2

[a] $R_1^{IS}{}_{(obs)}$ is the initial recovery of the selective spin–lattice relaxation measurements.

NOE difference spectra of d(CG)$_3$ in 4 M $NaClO_4$ exhibited strong interactions between GH8 and GH1′, in agreement with the assignment for the Z family (data not shown). In 0 M $NaClO_4$, cross-peak networks between aromatic and sugar H1′ were seen in the NOESY spectra of d(CG)$_3$, in agreement with the assignment for the B family (data not shown). In 2 M $NaClO_4$, we observed two sets of cross peaks in the NOESY spectra for the B and Z family d(CG)$_3$. These NOE experiments together with UV melting experiments and CD spectra confirm that d(CG)$_3$ in 2 M $NaClO_4$ exists as a mixture of the B and Z family of duplexes rather than a single-strand coil. Although two double-helical forms of d(CG)$_3$ in 2 M $NaClO_4$ need not completely match with idealized B- and Z-structures,[20] they belong at least to the B and Z family of double-helical DNAs.

(16) Wagner, G.; Wuthrich, K. *J. Magn. Reson.* **1970**, *33*, 675–680.
(17) Dobson, C. M.; Olejniczak, E. T.; Poulsen, F. M.; Ratcliffe, R. G. *J. Magn. Reson.* **1982**, *48*, 97–110.
(18) Clore, G. M.; Gronenborn, A. M. *FEBS Lett.* **1984**, *172*, 219–225.
(19) (a) Benight, A. S.; Wang, Y.; Amaratunga, M.; Chattopadhyaya, R.; Henderson, J.; Hanlon, S.; Ikuta, S. *Biochemistry* **1989**, *28*, 3323–3332. (b) Ikuta, S.; Chattopadhyaya, R.; Dickerson, R. E.; Kearns, D. R. *Biochemistry* **1986**, *25*, 4840–4848.
(20) Dickerson, R. E.; Drew, H. R.; Conners, B. N.; Wing, R. M.; Fratini, A. V.; Kopka, M. L. *Science* **1982**, *216*, 475–485.
(21) Wang, N. C.; Hogan, M. E.; Austin, R. H. *Proc. Natl. Acad. Sci. U.S.A.* **1982**, *79*, 5896–5900.

Table II. Rotating Frame Relaxation Rates ($R_{1\rho(obs)}$[a] and $R_{1\rho(exch)}$) of B- and Z-d(GC)$_3$ in 2 M $NaClO_4$ at 5 and 0 °C

5 °C				0 °C			
ω_1, Hz	$R_{1\rho(obs)}$, s^{-1}	$R_{1\rho(dd)}$, s^{-1}	$R_{1\rho(exch)}$, s^{-1}	ω_1, Hz	$R_{1\rho(obs)}$, s^{-1}	$R_{1\rho(dd)}$, s^{-1}	$R_{1\rho(exch)}$, s^{-1}
B-d(CG)$_3$, 3/5CH5							
2212	10.9	9.0	1.9	2212	15.4	10.8	4.6
5000	11.0	9.0	2.0	4393	15.2	10.8	4.4
5814	10.9	9.0	1.9	6410	14.9	10.8	4.1
7463	10.8	9.0	1.8	7463	14.8	10.8	4.0
Z-d(GC)$_3$, 3CH5							
2212	23.8	13.0	10.8	2212	32.3	16.4	15.9
5000	24.4	13.0	11.4				
5814	25.0	13.0	12.0	6410	28.6	16.4	12.2
7463	25.0	13.0	12.0	7463	27.0	16.2	10.6
Z-d(GC)$_3$, 5CH5							
2212	23.8	13.8	10.0	2212	31.3	17.2	14.1
5000	24.4	13.8	10.6	4393	29.4	17.2	12.2
5814	23.3	13.8	9.5	6410	27.8	17.2	10.6
7463	23.3	13.8	9.5	7463	26.3	17.2	9.1

[a] Errors have been estimated to be less than 5% for measurements of R_1 ($1/T_1$) and $R_{1\rho}(1/T_{1\rho})$.

Table III. Effective Two-Site Exchange Lifetimes (τ_{exch}) and Chemical Shift Differences ($\Delta\omega$) for Base Protons of B- and Z-d(CG)$_3$ in 10 mM phosphate buffer, 0.1 M NaCl, 2 M $NaClO_4$, and pH = 6.6 at 0 °C

	τ_{exch}, μs	$\Delta\omega$, ppm
B-d(CG)$_3$, 3/5CH5	≤10	≤0.8
Z-d(CG)$_3$, 5CH5	16.4	1.0
Z-d(CG)$_3$, 3CH5	16.2	1.1

$T_{1\rho}$ of B- and Z-d(CG)$_3$. Figure 3 shows $T_{1\rho}$ spectra from spin-locking experiments[9] for the CH5 of B- and Z-d(CG)$_3$ at 5 °C. $R_{1\rho(obs)}$ were 10.8 and 25.0 s^{-1} for the 3CH5 of B- and Z-d(CG)$_3$, respectively, at ω_1 = 7463 Hz. The 3CH5 of Z-d(CG)$_3$ relaxed faster than that of B-d(CG)$_3$. The initial recovery of the magnetization, $R_1^{IS}{}_{(obs)}$, in the selective T_1 experiments was 3.0 and 5.0 s^{-1} for B- and Z-d(CG)$_3$, respectively, (listed in Table I). The conformational exchange contribution, $R_{1\rho(exch)}$, for protons such as the CH5 and GH8 is the difference between $R_{1\rho(obs)}$ and $R_{1\rho(dd)}$ (see eq 1). As presented above, $R_{1\rho(dd)}$ was obtained from $R_1^{IS}{}_{(obs)}$ and theoretical ratios of $R_{1\rho(dd)}/R_1^{IS}{}_{(dd)}$. The ratios were 3.0 and 2.6 for B- and Z-d(CG)$_3$, respectively, calculated by using apparent correlation times (τ_{app}'s) that were measured by pre-steady-state NOE experiments (see below). $R_{1\rho(dd)}$ were found to be 9.0 and 13.0 s^{-1} for the 3CH5 of B- and Z-d(CG)$_3$, respectively. These led to $R_{1\rho(exch)}$ of 1.8 and 12.0 s^{-1} for the 3CH5 of B- and Z-d(CG)$_3$, respectively (Table II).

In an attempt to obtain τ_{exch} and $\Delta\omega$ for the conformational exchanges of interest, $T_{1\rho}$ were measured for the CH5 of B- and Z-d(CG)$_3$ with different spin-locking fields, ω_1, ranging from 2212 to 7463 Hz at 5 °C and analyzed as described above. These data are summarized in Table II. $R_{1\rho(exch)}$ were larger in Z-d(CG)$_3$ than in B-d(CG)$_3$ and were independent of ω_1.

In order to slow down the conformational exchanges, measurements of $T_{1\rho}$ were performed at 0 °C. $R_{1\rho(exch)}$ at 0 °C were larger than those of the corresponding signals at 5 °C (Table II). At this temperature, 0 °C, $R_{1\rho(exch)}$ of Z-d(CG)$_3$ were observed to vary inversely with ω_1: ~15 s^{-1} at 2212 Hz and ~10 s^{-1} at 7463 Hz. However, $R_{1\rho(exch)}$ of B-d(CG)$_3$ remained independent of ω_1 (Table II). $T_{1\rho(exch)}$ are plotted for the 5CH5 of Z-d(CG)$_3$ against ω_1^2, shown in Figure 4. A straight line was obtained as predicted by eq 3. From the slope $[4\tau_{exch}/(\Delta\omega)^2]$ and intercept $4/[(\Delta\omega)^2\tau_{exch}]$, τ_{exch} = 16.4 μs and $\Delta\omega$ = 1.0 ppm were obtained for the 5CH5 of Z-d(CG)$_3$. These data are listed in Table III. τ_{exch} of ~9 μs is estimated for the 5CH5 of Z-d(CG)$_3$ at 5 °C assuming that $\Delta\omega$ is temperature invariant. The increased $R_{1\rho(exch)}$ at 0 °C relative to $R_{1\rho(exch)}$ at 5 °C is due to the increase in τ_{exch}. These data demonstrate that (i) $T_{1\rho}$ detects the conformational exchanges occurring on the microsecond time scale and (ii) conformational exchange contributions are larger in Z-d(CG)$_3$ than in B-d(CG)$_3$ on this time scale.

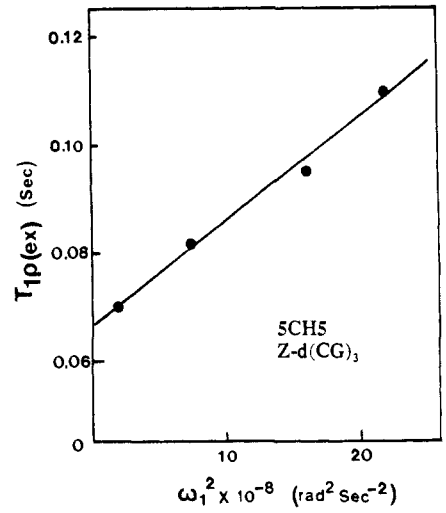

Figure 4. Plot of $T_{1\rho(exch)}$ for the 5CH5 of Z-d(CG)$_3$ obtained at 0 °C as a function of ω_1^2 at γB_0 = 300 MHz.

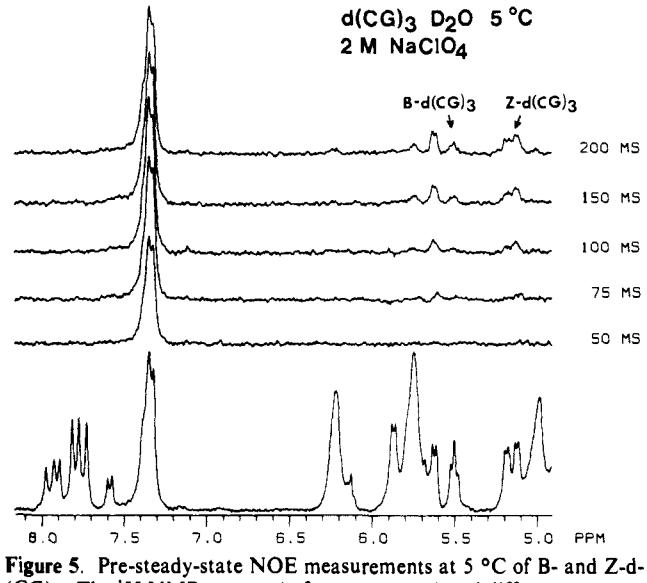

Figure 5. Pre-steady-state NOE measurements at 5 °C of B- and Z-d(CG)$_3$. The ^{1}H NMR spectra (reference spectra) and difference spectra (off-resonance minus on-resonance pre-saturation).

NOE and T_1 of B- and Z-d(CG)$_3$. A series of NOEs were measured at different irradiation times, t, ranging from 50 to 200 ms for the CH6→CH5 of B- and Z-d(CG)$_3$ at 5 °C. Results of the NOE experiments are shown in Figure 5. Up to 75 ms of irradiation, NOEs are near the noise level for both conformers. Irradiation for 100 ms results in an obvious NOE signal for Z-d(CG)$_3$, while B-d(CG)$_3$ does not give rise to an NOE signal until irradiated for 150 ms. Cross-relaxation rates, σ, are obtained from the initial slopes of NOE buildup profiles. σ are 0.4 and 0.9 s^{-1}, corresponding to τ_{app} of 1.7 and 3.6 ns for B- and Z-d(CG)$_3$, respectively. The presteady-state NOE experiments were also conducted at 0 °C and the results are summarized in Table I. The reader will note, from the data of Table I, that σ and τ_{app} of B-d(CG)$_3$ are about half the values of Z-d(CG)$_3$ at 0 and 5 °C.

Laboratory frame spin-lattice relaxation rates, $R_1^{IS}{}_{(obs)}$, were measured for the CH5 and were 3.0 and 5.3 s^{-1} at 5 °C for B- and Z-d(CG)$_3$, respectively. In the two-spin system a ratio of $R_1^{IS}{}_{(dd)}/\sigma$ for large molecules ($\omega\tau_c \gg 1$) approaches a theoretical ratio of 5.0 (see eq 5 and ref 15). The observed ratio of (3.0/0.4) = 7.5 and (5.3/0.9) = 5.9 for B- and Z-d(CG)$_3$, respectively, indicates that the CH5 relax mainly due to the CH6 and imply the contribution of the additional relaxation pathway to $R_1^{IS}{}_{(obs)}$ such as the CH5–H2″ for B-d(CG)$_3$ and the CH5–H2′ for Z-d(CG)$_3$.

Discussion

Microsecond Time Scale. Analysis of $T_{1\rho}$ measurements at 5 and 0 °C suggests the following: (i) both B- and Z-d(CG)$_3$ possess $R_{1\rho(exch)}$; (ii) the magnitude of $R_{1\rho(exch)}$ is significantly diverse (~4 s^{-1} for B-d(CG)$_3$ and ~15 s^{-1} for Z-d(CG)$_3$ with ω_1 = 2212 Hz at 0 °C); (iii) Z-d(CG)$_3$ has $R_{1\rho(exch)}$ 2–5 times larger than B-d(CG)$_3$; (iv) $R_{1\rho(exch)}$ for B- and Z-d(CG)$_3$ vary with temperature; and (v) the lifetime of the conformational exchange for Z-d(CG)$_3$ is brought into the $T_{1\rho}$ time scale window, to yield τ_{exch} and $\Delta\omega$ by lowering the temperature from 5 to 0 °C. This indicates that an activation barrier exists for the conformational exchanges.

The magnitude of $R_{1\rho nexch)}$ provides a measure of the conformational exchanges since it contains effects from both τ_{exch} and $\Delta\omega$ for the exchange process (eq 3). It is reasonable to assume that a larger $\Delta\omega$ correlates with greater amplitudes in the conformational exchanges.[8] Therefore, Z-d(CG)$_3$ possesses larger internal mobility than B-d(CG)$_3$ on this time scale.

An attempt was made to estimate the amplitude and lifetime of the conformational exchange. Measurements of $T_{1\rho}$ for an averaged sharp single line of the CH5 but not on the signal arising from directly exchanging species were conducted at different ω_1 fields. The chemical shift difference ($\Delta\omega$) between the exchanging sites and the lifetime (τ_{exch}) was extracted with use of a model with the two sites equally populated, described in Analysis of $T_{1\rho}$ Data. Although this model may be oversimplified for the conformational analysis of oligodeoxyribonucleotides, it provides first approximation information on the conformational exchange.[8] An accuracy of $\Delta\omega$ estimated by $T_{1\rho}$ measurements can be rigorously examined by comparing it with an experimentally observed $\Delta\omega$. This comparison will be made at the temperature at which the two signals arising from the corresponding sites are seen due to slow exchange. The rigorous examination of $\Delta\omega$ has been carried out for cis and trans isomerization of methyl nitrite by lowering temperature to −50 °C.[10] However, satisfactory spectra that exhibit signals arising from the exchanging species may not always be obtained for biological macromolecules dissolved in an aqueous solution due to a limitation in lowering temperatures below 0 °C: The hexamer, d(CG)$_3$, dissolved in an aqueous 2 M $NaClO_4$ solution is not an exception. The prediction of $\Delta\omega$, which otherwise could not be obtained, is unique and one of the advantages of $T_{1\rho}$ measurements.

The analysis of $T_{1\rho}$ relaxation data based on this model yields $\Delta\omega$ and τ_{exch}, independently. $\Delta\omega$ = 1.0 − 1.1 ppm and τ_{exch} = ~16 μs are obtained for Z-d(CG)$_3$, while $\Delta\omega \leq$ 0.8 ppm and $\tau_{exch} \leq$ 10 μs are obtained for B-d(CG)$_3$ (Table III and see below). These data clearly demonstrate that $T_{1\rho}$ measurements detect the kinetics of the conformational exchange occurring on the microsecond time scale. The larger $R_{1\rho(exch)}$ of Z-d(CG)$_3$ is associated with larger $\Delta\omega$ and τ_{exch} between the exchanging sites (eq 3). The conformational exchanges of Z-d(CG)$_3$ are larger in amplitude and slower than those of B-d(CG)$_3$ on the microsecond time scale. *Whether the difference in the conformational exchange kinetics between B- and Z-d(CG)$_3$ on the microsecond time scale might be characteristic near a B-to-Z transition region, 2 M $NaClO_4$, or occur even away from this region is currently under investigation.* We conclude that Z-d(CG)$_3$ is conformationally more mobile than B-d(CG)$_3$ *in 2 M $NaClO_4$* on this time scale. Physical models that account for the conformational exchanges include bending motions,[21] bending motions with a base pair opening,[22] or collective twisting motions.

The exchange lifetime of the B-to-Z transition is measured for d(CG)$_3$ by saturation transfer technique and is 3 s at 18 °C.[23] Such slow exchanges are outside the $T_{1\rho}$ time scale window, and therefore they cannot be detected by $T_{1\rho}$ measurements (see Figure 6 and the $T_{1\rho}$ time scale window).

$T_{1\rho}$ Time Scale Window. Theoretical values of $R_{1\rho(exch)}$ were calculated from eq 3 by using $\Delta\omega$ = 1.1 ppm as a function of τ_{exch} at different ω_1 (shown in Figure 6). Two exchange lifetimes of

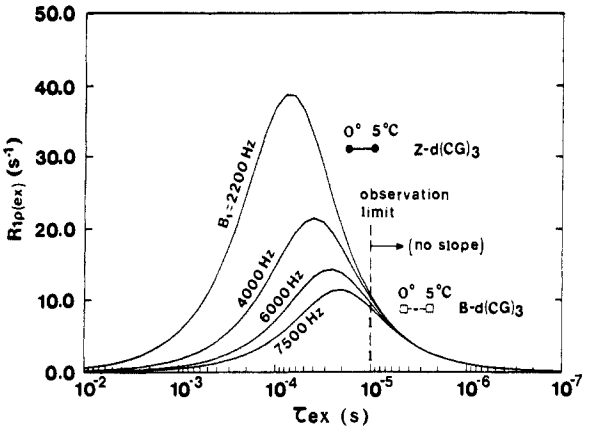

Figure 6. Theoretical values of $R_{1\rho(exch)}$ calculated by eq 3 using $\Delta\omega$ = 1.1 ppm (330 Hz) with different τ_{exch} and ω_1.

τ_{exch} = 16 μs at 0 °C and τ_{exch} = 9 μs at 5 °C for Z-d(CG)$_3$ are marked in this figure. It is evident that the observability of the variation in $T_{1\rho(exch)}$ with ω_1 is limited by the lifetime of τ_{exch} ~ 10 μs, in the present case. Conformational exchange contributes to $T_{1\rho}$ when τ_{exch} < 10 μs, but the variation in $T_{1\rho(exch)}$ with ω_1 is small and, therefore, within the experimental error of the NMR relaxation measurements. This is the case for B-d(CG)$_3$ at 0 and 5 °C and Z-d(CG)$_3$ at 5 °C. In contrast, with τ_{exch} > 10 μs the variation in $T_{1\rho(exch)}$ with ω_1 is large enough to be observed (Figure 6). As temperature was decreased from 5 to 0 °C, τ_{exch} for Z-d(CG)$_3$ increased from 9 to 16 μs and passed across the observability limit of τ_{exch} ~ 10 μs: $T_{1\rho(exch)}$ varied with ω_1. However, $T_{1\rho(exch)}$ of B-d(CG)$_3$ were independent of ω_1 even at 0 °C (Table II), indicative of τ_{exch} < 10 μs. The upper limit of $\Delta\omega$ for B-d(CG)$_3$ is estimated to be ~0.8 ppm from the limiting value of τ_{exch} = 10 μs. In order to further increase τ_{exch}, $T_{1\rho}$ measurements were carried out several times at −5 °C. Unfortunately, reliable relaxation data were not obtained due in part to the temperature near the freezing point of the sample dissolved in D_2O.

Nanosecond Time Scale. We previously reported the use of the NOE experiments to monitor the conformational exchange of CGCGCG stretches in a left-handed hairpin DNA[19a] and a left-handed hexadecamer, d(CGCGCGTATACGCGCG).[24] *The same technique has been used for studying the molecular dynamics of similar DNAs, d(CG)$_4$ and d(CG)$_6$.*[25] In the present study we observed that NOE buildup rates were very different for the short DNA duplexes with the identical sequence, CGCGCG, of different helical structure under the identical conditions. From the NOE buildup rates, the cross-relaxation rates, σ, were obtained. The σ values for B-d(CG)$_3$ were approximately a factor of 2 smaller than those of Z-d(CG)$_3$ at 0 and 5 °C (Table I). This leads to the τ_{app}'s of B-d(CG)$_3$ being approximately a factor of 2 smaller than those of Z-d(CG)$_3$ regardless of the accuracy of the estimation in the interproton distance as long as the identical interproton distance is used for B- and Z-d(CG)$_3$.

We try to explain the observation as simply as possible. *The line widths of NMR signals are sensitive to the size of the molecule and will serve as a marker of aggregations. The line widths of the GH8 are comparable, 6–8 Hz, for B- and Z-d(CG)$_3$ so that the preferential aggregation of Z-d(CG)$_3$ over B-d(CG)$_3$ is unlikely.* One of the simplest explanations is that B-d(CG)$_3$ is conformationally more mobile than Z-d(CG)$_3$ *in 2 M $NaClO_4$* on the nanosecond time scale. The possible motional model of the CH5→CH6 vector is out of plane motions.[2b]

Differential Mobilities. We have utilized both $T_{1\rho}$ and the pre-steady-state NOE to investigate the conformational exchanges of B- and Z-d(CG)$_3$ *in 2 M $NaClO_4$* solution. Each technique detects the conformational exchanges occurring on a characteristic

(22) Ramstein, J.; Lavery, R. *Proc. Natl. Acad. Sci. U.S.A.* **1988**, *85*, 7231–7235.
(23) Unpublished results.
(24) Ikuta, S.; Wang, Y. *Nucl. Acids. Res.* **1989**, *11*, 4131–4144.
(25) Eimer, W.; Williamson, J. R.; Boxer, S. G.; Pecora, R. *Biochemistry* **1990**, *29*, 799–811.

time scale: the microsecond time scale by $T_{1\rho}$ and the nanosecond time scale by the pre-steady-state NOE. NOE data indicate that B-d$(CG)_3$ is more mobile than Z-d$(CG)_3$ in 2 M $NaClO_4$ on the nanosecond time scale. However, $T_{1\rho}$ data indicate that the reverse is true on the microsecond time scale. Light-scattering experiments[26] and NMR proton-exchange studies[27] indicate that the B form is more mobile than the Z form and support our NOE results.

It is evident from our $T_{1\rho}$ and NOE results that B- and Z-d$(CG)_3$ each have different internal mobilities on different time scales. To our knowledge, this is the first observation that the degree of the internal mobilities of biological macromolecules is reversed in different time domains.

Acknowledgment. We thank Drs. G. Brubaker, V. Hsu, and H. Zabin for helpful discussion and suggestions and the anonymous referees for the critical and constructive comments on the manuscript. We also thank Ms. Y. Shi for assistance in drawing Figure 6. This research was supported by the Research Corporation, PHSBRSG No. 2SO7RR727-23, and the American Cancer Society, Illinois Division Grant No. 88-47.

(26) Thomas, T. J.; Bloomfield, V. A. *Nucl. Acids Res.* **1983**, *11*, 1919-1930.
(27) Mirau, P. A.; Kearns, D. R. *Proc. Natl. Acad. Sci. U.S.A.* **1985**, *82*, 1594-1598.

Histidinol Dehydrogenase: ^{18}O Isotope Shift in ^{13}C NMR Reveals the Origin of Histidine Oxygens

Charles Timmis Grubmeyer* and Salvatore Insinga

Contribution from the Department of Biology, New York University, 100 Washington Square, New York, New York 10003. *Received November 6, 1989*

Abstract: The reaction catalyzed by L-histidinol dehydrogenase (EC 1.1.1.23) is the unusual NAD-linked 4-electron oxidation of L-histidinol carried out by way of an unknown aldehyde level intermediate that is covalently linked to the enzyme. Proposals have included an imine derivative of an active site lysine. The ^{18}O isotope shift in ^{13}C NMR was used to investigate the origin of the two oxygens in product histidine. Histidinol dehydrogenase from *Salmonella typhimurium* was incubated with highly enriched L-[hydroxymethyl-^{13}C]histidinol with NAD in 50% $H^{18}OH$; an NAD regenerating system was used to maintain high levels of NAD. Direct examination of the product L-[carboxy-^{13}C]histidine in ^{13}C NMR revealed two peaks separated by 0.02 ppm, indicative of incorporation of a single solvent oxygen. The failure to expel the original histidinol oxygen provides evidence against the participation of an imine in the reaction pathway.

The reaction catalyzed by L-histidinol dehydrogenase (HDH; EC 1.1.1.23) is a 4-electron oxidation of the amino alcohol substrate by two molecules of NAD to produce histidine, the final step in the bacterial,[1] fungal,[2] and plant[3] biosyntheses of this amino acid. The enzyme from *Salmonella typhimurium*[4] has been most widely studied. The key mechanistic problem posed by HDH is the chemistry of the aldehyde-level intermediate. Here, we use the ^{18}O perturbation of ^{13}C chemical shifts[5] to find that product histidine contains only a single solvent oxygen, demonstrating that formation of the intermediate does not expel the original histidinol oxygen, and ruling out an intermediate imine.

Externally added synthetic histidinaldehyde is chemically and kinetically competent to be the partially oxidized intermediate in the HDH reaction; however, during the overall oxidation of histidinol, histidinaldehyde is neither released to the medium nor accessible to aldehyde derivatizing reagents.[1] Gorisch and Holke[6] have shown that added histidinaldehyde is bound very tightly to HDH ($K_D = 1.4 \times 10^{-11}$ M), with $k_{off} = 2.6 \times 10^{-5}$ s^{-1}, and is protected in its bound form from degradation by solvent. These observations have led to the hypothesis that the intermediate is covalently bound to the protein.[1,6,7] Several proposals have been made[6-8] that an imine derivative of an active site lysine occurs, as demonstrated for uridine 1,6-diphosphoglucose dehydrogenase (UDPGDH, EC 1.1.1.22), another 4-electron dehydrogenase;[9] a thiohemiacetal has also been suggested for both enzymes.[7,8,10] The imine intermediate is attractive given the ease of formation and analogy with UDPGDH; however, the chemistry of an imine intermediate does not suggest a mechanistic route for the second oxidation. Chemically, a thiohemiacetal provides a plausible route for an NAD-linked oxidation to a thiolester, followed by hydrolytic cleavage to produce the product acid. The mechanism of the aldehyde oxidation step is of general interest, since aldehyde dehydrogenases are thought in general to use thiohemiacetals, although cysteine modification of human mitochondrial aldehyde dehydrogenase does not abolish activity.[11]

As shown in Scheme I, formation of the imine of histidinaldehyde would expel the original oxygen atom of histidinol leading to histidine product containing two solvent oxygens; the thiohemiacetal mechanism does not predict loss of the histidinol oxygen. Thus, by performing the HDH reaction in $H^{18}OH$ and analyzing the isotopic composition of the product one can distinguish these possibilities. Such oxygen expulsion has been observed in the case of fructose-1,6-phosphate aldolase.[12] The laboratory of Van Etten has detailed the upfield isotope shift caused by ^{18}O on the NMR chemical shift of adjacent ^{13}C atoms,[5] an effect that is additive in multiply substituted carbon atoms.[13] The same group has also demonstrated that this technology can be used to study reaction pathways.[14] Here, we investigated the

(1) Adams, E. *J. Biol. Chem.* **1955**, *217*, 325-344.
(2) Keesey, J. R.; Bigelis, R.; Fink, G. R. *J. Biol. Chem.* **1979**, *254*, 7427-7433.
(3) Miflin, B. J.; Lea, P. J. In *Encyclopedia of Plant Physiology*; Pirson, A., Zimmermann, M. H., Eds.; Springer-Verlag: New York, 1982; Vol 14A, p 39.
(4) Loper, J. C.; Adams, E. *J. Biol. Chem.* **1965**, *240*, 788-795.
(5) Risley, J. M.; Van Etten, R. L. *J. Am. Chem. Soc.* **1979**, *101*, 252-253.
(6) Gorisch, H.; Holke, W. *Eur. J. Biochem.* **1985**, *150*, 305-308.
(7) Eccleston, E. D.; Thayer, M. L.; Kirkwood, S. *J. Biol. Chem.* **1979**, *254*, 11399-11404.
(8) Burger, E.; Gorisch, H. *Eur. J. Biochem.* **1981**, *118*, 125-130.
(9) Ordman, A. B.; Kirkwood, S. *J. Biol. Chem.* **1977**, *252*, 1320-1326.
(10) Ridley, W. P.; Houchins, J. P.; Kirkwood, S. *J. Biol. Chem.* **1975**, *250*, 8761-8767.
(11) Hempel, J. D.; Pietruszko, R. *J. Biol. Chem.* **1981**, *2576*, 10889-10896.
(12) Model, P.; Ponticorvo, L.; Rittenberg, D. *Biochemistry* **1968**, *7*, 1339-1347.
(13) Risley, J. M.; Van Etten, R. L. *J. Am. Chem. Soc.* **1981**, *103*, 4389-4392.
(14) Mega, T. L.; Van Etten, R. L. *J. Am. Chem. Soc.* **1988**, *110*, 6372-6376.

0002-7863/90/1512-5906$02.50/0